STRUCTURE AND PROPERTIES OF DLC LAYERS FOR INDUSTRIAL APPLICATIONS

MATES Tomáš[1], LEDINSKÝ Martin[1], VETUSHKA Aliaksei[1], PIKNA Peter[1], FEJFAR Antonín[1], MAREK Aleš[2], VYSKOČIL Jiří[2], ERICHSEN Jörn[3], DAWAH Patrick[3]

[1]Institute of Physics AS CR, v.v.i., Prague, Czech Republic, EU
[2]HVM Plasma, spol. s r.o., Prague, Czech Republic, EU
[3]Continental Mechanical Components Germany GmbH, Roding, Germany, EU

Abstract

Diamond-like carbon (DLC) layers based on amorphous carbon are used for wide range of applications, mostly for mechanical protection of various industrial components. As the properties of DLC layers are closely linked to their structure, we examined them at micro- and nanoscale by two independent microscopic techniques: Scanning Electron Microscopy (SEM) and Atomic Force Microscopy (AFM) with a good agreement. We compared DLC layers grown on steel substrate and Si wafer and found similarly structured clusters with hundreds of nm in diameter and a certain difference in the density of nucleation centres for each substrate. The measurements of local mechanical properties by the AFM tip revealed that the Si wafer behaves as softer material compared to the growing DLC nanoclusters that also exhibit lower values in the map of the relative local friction coefficient. Finally, we observed changes in the Raman spectra of the DLC exposed to annealing at ambient conditions and found a gradual shift from the diamond phase to the graphite phase as a function of increasing temperature. At the highest temperature of 400°C we observed the formation of tungsten oxide from an additional element contained in the multi-layer stack.

Keywords: DLC, PACVD, AFM, SEM, Raman

1. INTRODUCTION

DLC layers are frequently used for mechanical protection of various industrial components. Apart from high hardness and low friction coefficient, these layers exhibit also other interesting properties (optical, electrical, biological etc.) leading to much wider range of applications [1]. DLC layers actually represent a larger variety of structures based on amorphous carbon, with or without hydrogen and possibly with additional metallic or non-metallic components [2]. In this paper we solely focus on a selected type of DLC layer, i.e. hydrogenated amorphous carbon (a-C:H), which is currently used in certain automotive applications as a wear resistant layer. For the sake of its further optimisation, we studied its micro- and nanoscale structure and local mechanical properties and also its stability to elevated temperatures and compare our results with the published data.

2. EXPERIMENTAL

The DLC layers in this study were prepared by Plasma Assisted Chemical Vapour Deposition (PACVD) method in a commercial deposition system HTC-1500 by Hauzer Techno Coating. Additionally, PACVD was combined with magnetron sputtering, where graphite-tungsten alloy and pure chromium targets were used. Precursor gas was acetylene (C_2H_6) at the pressure of 10^{-1} Pa. The substrate temperature within the whole deposition process was kept below 200°C. For a proper adhesion of rather thick DLC layer (3.2 µm), a common multi-layer structure (Cr adhesion layer and a-C:H:W stress buffer layer, for details see e.g. [3]) was applied. Silicon wafer and polished steel were used as substrates.

The surface of the DLC layers was measured with the Scanning Electron Microscope (SEM) TESCAN MAIA 3 equipped with Schottky emitter, using 5 kV acceleration voltage and ~5 mm working distance.

For further surface details, including the maps of local mechanical properties, two Atomic Force Microscopes (AFM) operated under ambient conditions were used. The maps of local friction were measured by Veeco (Bruker) Dimension 3100 AFM with NanoScope IV controller, operated in contact mode with the detection of lateral forces acting on soft ContDLC probes with 13 kHz resonant frequency and 0.2 N/m force constant. For the maps of adhesion force and energy dissipation we used Bruker Dimension Icon AFM in PeakForce QNM mode [4] with more rigid Multi75DLC probes with 75 kHz resonant frequency and 3 N/m force constant. Both probes by BudgetSensors had tips with 15 nm DLC coating combining higher wear resistance compared to uncoated Si probes with still relatively sharp tip (radius < 15 nm) for a good image resolution.

The Raman spectra were measured in the back-scattering geometry using micro-spectroscopic Raman setup (InVia REFLEX by Renishaw) equipped with the blue excitation laser (442 nm / 100 mW). The inspected area (laser spot) had ~3 µm in diameter for the 50× objective with numerical aperture of 0.5. The spectra were fitted by Gaussian functions for both characteristic D and G peaks around 1360 and 1560 cm^{-1} respectively [5].

The annealing test of DLC layers deposited on steel substrates was performed in a high temperature oven under ambient conditions (no vacuum) at the specified temperature for a fixed duration of 4 hours.

3. RESULTS

Larger fields of view (e.g. hundreds of µm [6]) show the surface of DLC layers as very smooth and with no remarkable features. Therefore we focused to smaller fields of view (**Figures 1-3**), where a particular type of structure could be already observed and where a comparison between SEM and AFM images could be performed. The surface of the 3.2 µm thick DLC layers shows a continuous coverage with surface features in the shape of apparently smooth spherical caps (let us call them clusters) having straight boundaries among them. These boundaries are actually polylines defining the mutual contact areas among the clusters. The SEM topography images of the DLC layer deposited on steel substrate in **Figure 1a** and on Si wafer in **Figure 1b** look very much alike at the first sight. However, a closer look at the real dimensions, reveals certain difference in the normalized density of the nucleation centres on Si wafer (around 15-20 per 1x1 $µm^2$) compared to the steel substrate (around 3-5 per 1x1 $µm^2$). As a consequence, the DLC clusters grown on Si wafer are smaller (200 to 500 nm) compared to the clusters on the steel substrate (400 to 800 nm), which is also leads to a difference in the surface roughness by a factor up to 10 for these two particular substrates [6].

Further detailed measurements of the surface by SEM were carried out on the Si wafer substrate. Here we obtained a possibility to inspect the whole thickness variation (from the nucleation on the bare substrate towards the full layer thickness) within one sample. This feature was created in the vicinity of a clamp used to fix the sample during the deposition process. As we moved the sample along one axis in the SEM chamber, we crossed the thickness transition and therefore could obtain surface images for different film thicknesses. Three representative images for a smaller field of view of 2x2 $µm^2$ are shown in **Figures 1b-d.**

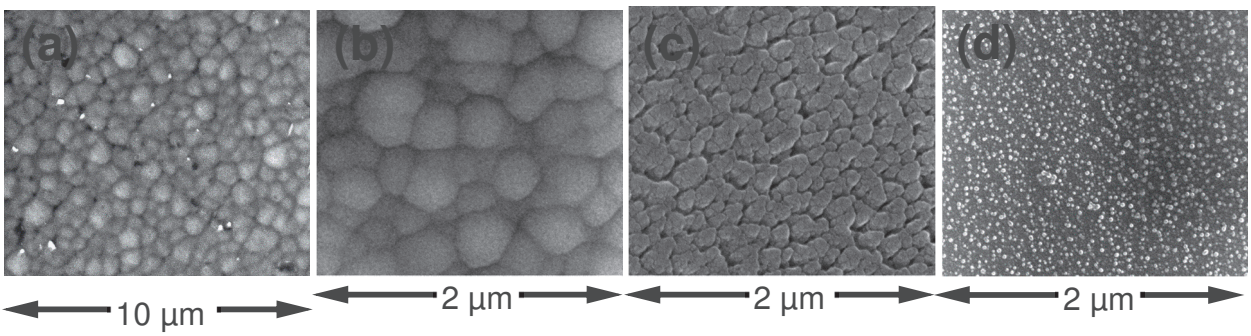

Figure 1 SEM images showing the surface structure of the DLC layer deposited on steel substrate (a) and on Si wafer at different growth stages: (b) final surface at the full thickness of 3.2 µm, (c) transition structure at the thickness of ~1 µm, (d) nucleation phase at ~30 nm

Figure 1b shows the surface at the full film thickness. The image in **Figure 1c** represents a thinner layer of ~1 µm with smaller clusters of different shapes - partly joined and partly still isolated with visible separation gaps. The rightmost image in **Figure 1d** shows the very early stage of growth, where only isolated clusters in the shape of nanoballs are to be found. A more detailed analysis of the three sub-images of **Figures 1b-d** reveals that the number of clusters per normalized area (1x1 µm^2) is clearly different for each thickness. Specifically, we identified ~25 clusters for the 3.2 µm thick layer, ~100 clusters for the ~1 µm thick layer and ~200 clusters for the 30 nm thick layer, always for the same normalized area.

We continued our study with the same sample (DLC layer with the thickness transition on Si wafer substrate) in the AFM microscope. The first image in **Figure 2a** represents the 3.2 µm thick layer and its surface topography for the same field of view 2x2 µm^2 as in **Figure 1b.** This comparison shows a perfect agreement of results obtained by two independent microscopic techniques (SEM and AFM) based on different sensing principles.

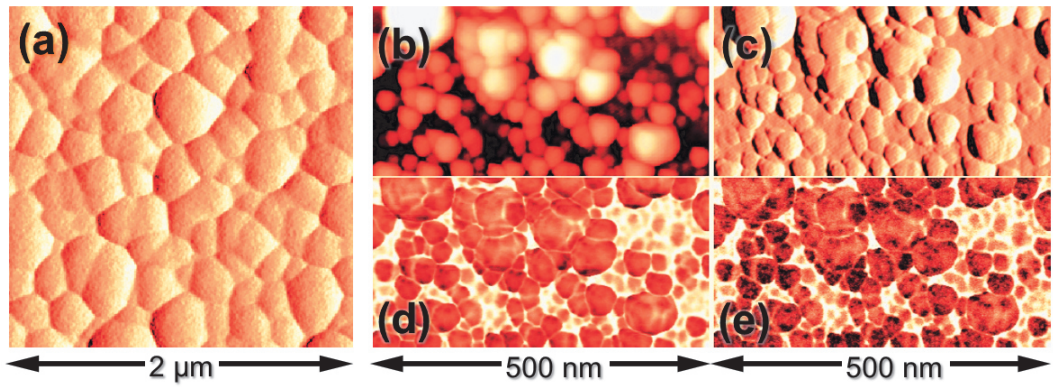

Figure 2 Structure of the DLC layer by AFM showing (a) topography at full thickness of 3.2 µm, (b) local height, (c) topography, (d) adhesion and (e) dissipation for the ~30 nm thickness

The other four sub-images of **Figure 2** show a smaller area (500 x 250 nm^2) of the thinnest part of the DLC layer with 30 nm thickness observed already in **Figure 1d**. As we employed the novel PeakForce QNM measurement mode, we could obtain not only conventional images of local height (**Figure 2b**) and topography (**Figure 2c**), but also local mechanical properties like adhesion (**Figure 2d**) and energy dissipation (**Figure 2e**). Both maps of local adhesion and dissipation indicate that the Si wafer behaves as softer material (brighter areas) compared to the DLC clusters (darker areas) during the contact with the probing tip. These maps of local mechanical properties provide an illustrative material contrast that helps to distinguish between the Si substrate and the DLC clusters more easily (which would be a bit more difficult when having just the topography images).

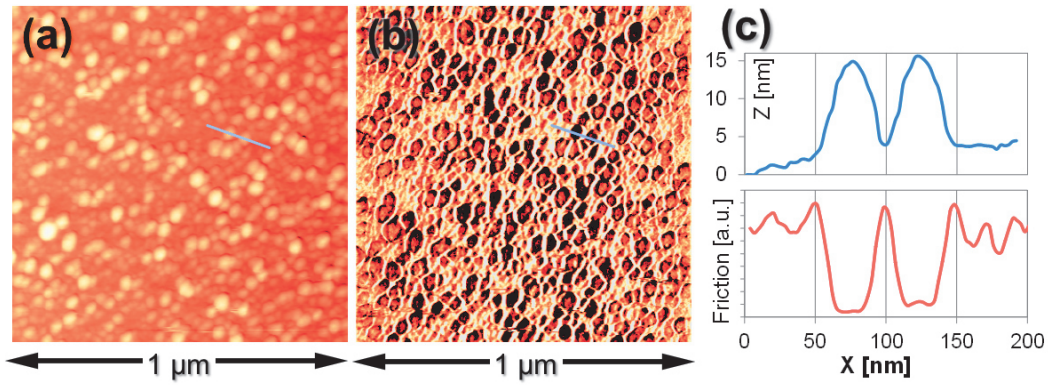

Figure 3 Local height (a) and local friction map (b) with representative line profiles (c) by Lateral Force Microscopy showing lower friction (darker spots in (b)) of the DLC clusters in the nucleation phase at~30 nm

Further characterization of the mechanical properties at nanoscale were carried out by the common contact AFM mode, which allows the detection of the friction force from the torsion bending of the soft cantilever pulled over the inspected area. This torsion bending is proportional to the friction coefficient between the surface and the AFM tip. However, for rough surfaces additional contributions from topography may appear in the local friction images. In order to eliminate these artefacts, we performed 2 scans in opposite scan directions and processed the data into one image, shown in **Figure 3b** together with the corresponding local height image in **Figure 3a**, for the same spot as in **Figures 2b-e**. Illustrative line profiles over two small DLC clusters at positions of 80 and 120 nm in **Figure 3c** show smaller local friction values for the DLC clusters compared to the Si wafer.

Some applications may require the utilization of thicker DLC layers (few µm), where the high values of internal stress may cause issues with the layer adhesion. This could be partly addressed by additional adhesive layers and/or by a suitable post-deposition annealing treatment [7, 8], where the allowed temperature range should be known. Therefore, we conducted the annealing experiment in air for the DLC layers prepared on steel substrates and for temperatures up to 400°C. As a feedback signal, we checked the Raman spectra (**Figure 4**), which are frequently reported in the literature too.

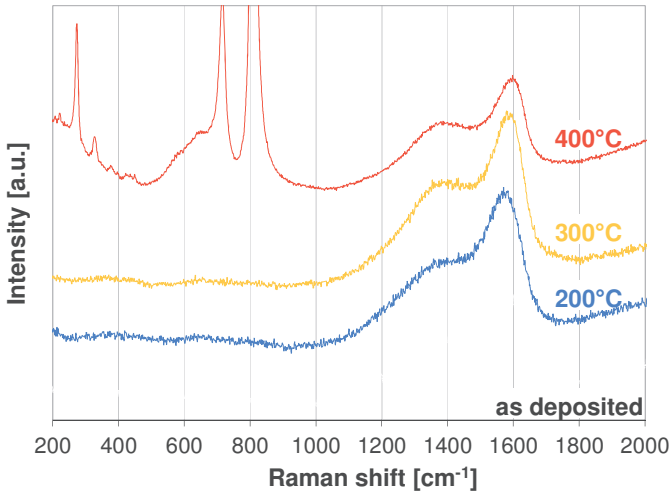

Figure 4 Raman spectra of DLC layers on steel substrates as a function of the annealing temperature

From the evaluated data we observed a certain shift both for the G peak position and for the I(D)/I(G) ratio as a function of the annealing temperature (**Figure 5**). At the highest annealing temperature of 400°C we observed the formation of 4 new additional sharp peaks in the range from ~300 to ~800 cm^{-1}.

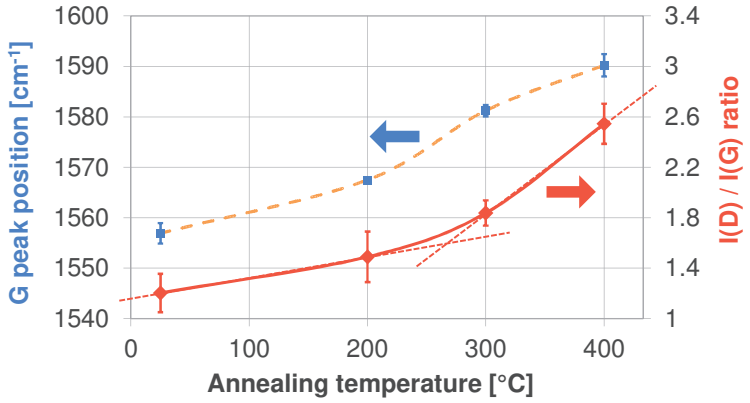

Figure 5 Evaluated Raman spectra from **Figure** 4 showing G peak position and I(D)/I(G) ratio

4. DISCUSSION

During the study of surface structures of DLC layers we found a very good agreement between the data from SEM and AFM microscopes for the field of view 2x2 μm^2 (see **Figure 1b** vs **Figure 2a**), which confirms their trustworthiness. In both cases the typical measurements artefacts (charging of poorly conductive sample for SEM and blunt tip for AFM) were suppressed. The network of smooth clusters separated by polylines is a typical product of the 3D island growth mode, where the centres of the clusters would represent the nucleation spots at the layer/substrate interface. Similar growth mode was previously observed and described for a different material - μc-Si:H grains in a-Si:H matrix [9]. Detailed comparison of the apparent density of nucleation spots (derived from the surface images at different layer thicknesses in **Figure 1**) leads to a conclusion that besides the normal 3D island (Volmer-Weber) growth mode, the clusters also must have undergone a certain process of coalescence, which is in agreement with other studies [10] and the references therein.

The material contrast observed in **Figures 2d** and **2e** for the isolated DLC clusters is certainly welcome additional information for the interpretation of topographic data. Both values of local adhesion force and energy dissipation represent somehow bound information about the attractive interaction between tip and surface during the tip retraction. The appealing interpretation would consider the Si wafer being a softer material allowing the tip to penetrate deeper, therefore creating a larger contact area, which leads to a higher adhesion force measured afterwards. However, there is also other, less attractive, interpretation based on the effect of the capillary meniscus. DLC layers are known to be close to the hydrophobic / hydrophilic boundary [11, 12], while the Si wafer (with a layer of native oxide) is definitely more hydrophilic. Therefore a larger meniscus would be formed on the Si wafer, leading to higher attractive forces, which might be also the source of the contrast observed in the maps of adhesion force and energy dissipation.

Luckily, the local friction data (**Figure 3**) provide a more straightforward interpretation, which is consistent with the tribological data published for the macroscale experiments. Friction coefficients up to 0.7 for Si in air [13], while only 0.1 - 0.2 for the DLC layers [3, 8, 12] were reported. Therefore we could also conclude that the macroscale (see literature) and nanoscale (see **Figure 3c**) tribological properties of Si and DLC are analogous.

The trends of G-peak position and I(D)/I(G) ratio in **Figure 5** are consistent with similar annealing experiments published earlier [7, 8, 14]. Although the data in **Figure 5** may significantly correlate with the relative contents of the diamond or graphite phase in the DLC layer, this may not be a monotonous function [11] and so additional diagnostics methods are needed to verify this. A very clear trend of the DLC layer hardness shown in [8], together with similar set of Raman spectra, allows us to conclude that the transition from a hard layer (with pronounced diamond phase) to a softer layer (dominant graphite phase) occurred between the temperatures of 200 and 300°C. The change of slope of I(D)/I(G) ratio vs temperature (dotted lines in **Figure 5**) visualizes this transition. The additional sharp peaks at 272, 326, 714 and 809 cm^{-1} were identified as tungsten oxide (WO_x) [15] formed during the annealing in air (O supply) and in the presence of the a-C:H:W sublayer (W supply).

5. CONCLUSION

We explored the structure of DLC layers from industrial applications, which were prepared for our study on steel and Si wafer substrates. We found indications of the 3D island growth mode. At the nanoscale, we detected different local mechanical properties (adhesion, local friction) between the DLC nanoclusters and Si substrate using special AFM measurement modes. Finally, we verified that our hydrogenated DLC layers are stable up to around 200 °C, which should be taken into account during the further layer optimization.

ACKNOWLEDGEMENTS

The authors would like to thank Mgr. Pavla Bauerová for the measurement of SEM images. This work was partly funded by the HVM Plasma, s.r.o. and by the MEYS CR Project LM2015087.

REFERENCES

[1] VETTER, J. 60 years of DLC coatings: Historical highlights and technical review of various DLC types, and their evolution for industrial applications. *Surface & Coatings Technology*, 2014, vol. 257, pp. 213-240.

[2] BEWILOGUA, K., HOFMANN, D. History of diamond-like carbon films - From first experiments to worldwide applications. *Surface & Coatings Technology*, 2014, vol. 242, pp. 214-225.

[3] SOLIS, J. et al. Tribological performance of an H-DLC coating prepared by PECVD. *Applied Surface Science*, 2016, vol. 383, pp. 222-232

[4] FOSTER, B. New Atomic Force Microscopy (AFM) Approaches Life Sciences Gently, Quantitatively, and Correlatively. *American Laboratory*, 2012, vol. 44, no. 4, pp. 24-28.

[5] CASIRAGHI, C., FERRARI, A.C., ROBERTSON, J. Raman spectroscopy of hydrogenated amorphous carbons. *Physical Review B*, 2005, vol. 72, pp. 085401

[6] JELINEK, M. et al. Chromium-doped DLC for implants prepared by laser-magnetron deposition. *Materials Science and Engineering C*, 2015, vol. 46, pp. 381-386

[7] FRANTA, D. et al. Correlation of thermal stability of the mechanical and optical properties of diamond-like carbon films. *Diamond and Related Materials*, 2007, vol. 16, pp. 1331-1335

[8] HUANG, L. et al. Influence of annealing temperature on thermal stabilities of hydrogenated amorphous carbon on silicon nitride balls. *Vacuum*, 2016, vol. 127, pp. 96-102

[9] FEJFAR, A. et al. Model of electronic transport in microcrystalline silicon and its use for prediction of device performance. *Journal of Non-Crystalline Solids*, 2004, vol. 338-340, pp. 303-309

[10] CATENA, A. et al. Surface morphology and grain analysis of successively industrially grown amorphous hydrogenated carbon films (a-C:H) on silicon. *Applied Surface Science*, 2015, vol. 347, pp. 657-667

[11] ROBERTSON, J. Diamond-like amorphous carbon. *Materials Science and Engineering: R: Reports*, 2002, vol. 37, pp. 129-281.

[12] MEUNIER, C. et al. Friction properties of ta-C and a-C:H coatings under high vacuum. *Surface & Coatings Technology*, 2005, vol. 200, pp. 1976-1981

[13] BHUSHAN, B., LI, X. Micromechanical and tribological characterization of doped single-crystal silicon and polysilicon films for MEMS devices. *Journal of Materials Research*, 1997, vol. 12, pp. 54-63

[14] TALLANT, D.R., PARMETER, J.E., SIEGAL, M.P., SIMPSON, R.L. The thermal stability of diamond-like carbon. *Diamond and Related Materials*, 1995, vol. 4, pp. 191-199.

[15] SANTATO, C., et al. Crystallographically Oriented Mesoporous WO_3 Films: Synthesis, Characterization, and Applications. *Journal of the American Chemical Society*, 2001, vol. 123, pp. 10639-10649